

Joint Acceptance Attenuation Factor of Integrated Pressure with Unsteady Pressure-Sensitive Paint Measurements

Jie Li¹, Marc A. Shaw-Lecerf², David D. Murakami², E. Lara Lash², Nettie H. Roozeboom², Paul G. Bremner³

¹Metis Technology Solutions, Inc.
Moffett Field, CA 94035

²NASA Ames Research Center
Moffett Field, CA 94035

³AeroHydroPLUS
Del Mar, CA 92014

The Unsteady Pressure-Sensitive Paint (uPSP) is widely used to measure the surface pressure of scaled models in wind tunnel tests. Compared to the conventional pressure transducers, uPSP has the advantage of high spatial resolution. With multiple high-speed Complementary Metal Oxide Superconductor (CMOS) cameras, the uPSP data collected with the camera pixels are mapped to the surface grid of the scaled model and converted to pressure. The shot noise is the dominant component of the noise in the uPSP measurement. The integrated pressure is usually computed on the grid nodes of a user-defined patch. The effect of shot noise is reduced in the integrated pressure on the patch; however, the measurement of the aerodynamic pressure may also be attenuated by the decorrelation of the flow pressure field being measured. This paper discusses the Joint Acceptance Attenuation Factor (JAAF) of the integrated pressure with uPSP measurements. The JAAF, a function of frequency, is defined as the ratio of the Power Spectral Density (PSD) of the integrated aerodynamic pressure on the patch to the average PSD of the aerodynamic pressure on the grid nodes of the patch. In this paper, the JAAF is investigated for the integrated pressure on rectangular patches, whose edges are defined in the direction along the streamline or across the streamline. Based on the assumption that the surface pressure field can be described by the Corcos model, the closed-form formulas to compute the JAAFs of the integrated pressure on the discrete grid nodes of a rectangular patch and over the continuous area of a rectangular patch are derived respectively. It is shown that the JAAF of the integrated pressure over the continuous area of a rectangular patch is the limit of that on discrete nodes of the rectangular patch when the number of nodes in each row or column goes to infinity. The closed-form formulas of the JAAF derived in this paper, with estimated parameters of the model, are verified with the measurements of the uPSP and the conventional pressure transducer collected in the Space Launch System Ascent Unsteady Aerodynamics Test at NASA Ames Research Center in November 2017. The closed-form formulas of the JAAF of the integrated pressure on the rectangular patches, based on the Corcos model, provide an efficient method to estimate the attenuation of integration by the decorrelation of the flow pressure field and set references for the comparison of the spectrum of the integrated uPSP measurements and the conventional pressure transducer measurements. The work described in this paper is a part of NASA's development of a new state-of-the-art uPSP capability in production wind tunnels. Funding was provided by the NASA Aerosciences Evaluation and Test Capabilities Portfolio Office.

Nomenclature

AETC	= NASA Aerosciences Evaluation and Test Capabilities
AUAT	= Ascent Unsteady Aerodynamics Test
CMOS	= Complementary Metal Oxide Superconductor
CPSD	= Cross Power Spectral Density

c_x, c_y	= coefficients of the Corcos model to represent the decay of the surface pressure correlation in the directions along the streamline and across the streamline respectively
f	= frequency
i	= imaginary unit
JAAF	= Joint Acceptance Attenuation Factor
$J_{L \times W}(f)$	= JAAF of the integrated pressure over the continuous area of a rectangular patch with length L and width W
$J_{m \times n}(f)$	= JAAF of the integrated pressure on an $m \times n$ two-dimensional array of discrete grid nodes
$J_{x,L}(f), J_{y,W}(f)$	= JAAFs, in the directions along the streamline and across the streamline respectively, of the integrated pressure over the continuous area of a rectangular patch with length L and width W
$J_{x,n}(f), J_{y,m}(f)$	= JAAFs, in the directions along the streamline and across the streamline respectively, of the integrated pressure on an $m \times n$ two-dimensional array of discrete grid nodes
k_c	= convection wavenumber
L	= length of a rectangular patch
m, n	= number of rows and columns of a two-dimensional array of discrete grid nodes
PSD	= Power Spectral Density
$Re(z)$	= real part of a complex number z
SLS	= Space Launch System
U_c	= convection velocity
uPSP	= Unsteady Pressure-Sensitive Paint
UPWT	= NASA Unitary Plan Wind Tunnel
USA	= Universal Stage Adapter
W	= width of a rectangular patch
\bar{z}	= conjugate of a complex number z
α	= angle of attack
β	= angle of sideslip
δ_x, δ_y	= distance between two neighbor grid nodes in the directions along the streamline and across the streamline respectively
$\sum_{element} \Phi$	= sum of all elements of a matrix Φ
$\Phi_{CPSD, m \times n}$	= CPSD matrix of the pressure measurements on an $m \times n$ two-dimensional array of discrete grid nodes
$\phi_{CPSD}(\Delta x, \Delta y; f)$	= CPSD of the pressure at two points in a homogeneous surface pressure field, where Δx and Δy are components of the displacement between the two points along the streamline and across the streamline respectively
$\phi(f)$	= PSD of the pressure at a point in a homogeneous surface pressure field
$\phi_{i_1 j_1, i_2 j_2}$	= CPSD of the pressure measurements on the nodes $i_1 j_1$ and $i_2 j_2$ of an $m \times n$ two-dimensional array of discrete grid nodes
$\phi_{PSD, L \times W}(f)$	= PSD of the integrated pressure over the continuous area of a rectangular patch with length L and width W
$\phi_{PSD, m \times n}(f)$	= PSD of the integrated pressure on an $m \times n$ two-dimensional array of discrete grid nodes

I. Introduction

The Unsteady Pressure-Sensitive Paint (uPSP) is widely used to measure the surface pressure of scaled models in wind tunnel tests (Refs. [1]-[4]). Compared to the conventional pressure transducers, uPSP has the advantage of high spatial resolution. With multiple high-speed Complementary Metal Oxide Superconductor (CMOS) cameras, the uPSP data collected with the camera pixels are mapped to the surface grid of the scaled model and converted to pressure (Refs. [5]-[10]). The shot noise, which is associated with the quantum processes both in the generation of the photons by the luminescent uPSP and in the conversion of the photons into electrons within the camera, is the dominant component of the noise in the uPSP measurement. The standard deviation of shot noise of each pixel is proportional to the square root of the uPSP intensity measured with the pixel. The integrated pressure is usually computed as an area-weighted average of the uPSP measured pressure on the grid nodes of a user-defined patch area of the model.

Considering the shot noise is uncorrelated with the aerodynamic pressure and the shot noise of the uPSP data collected with different pixels is also uncorrelated, the effect of shot noise is reduced in the integrated pressure on the patch; however, the measurement of the aerodynamic pressure may also be attenuated by the decorrelation of the flow pressure field being measured (Refs. [11]-[14]).

This paper discusses the Joint Acceptance Attenuation Factor (JAAF) of the integrated pressure with uPSP measurements. The JAAF, a function of frequency, is defined as the ratio of the Power Spectral Density (PSD) of the integrated aerodynamic pressure on the patch to the average PSD of the aerodynamic pressure on the grid nodes of the patch (Refs. [15-17]).

In this paper, the JAAF is investigated for the integrated pressure on rectangular patches, whose edges are defined in the direction along the streamline or across the streamline. The paper is organized as follows. The model of the surface pressure field is described in Section 2. In Section 3, the JAAF of the integrated pressure on the discrete grid nodes of a rectangular patch is discussed and the closed-form formulas to compute the JAAF are derived. In Section 4, the closed-form formulas of the JAAF of the integrated pressure over the continuous area of a rectangular patch are derived, and it is shown that the JAAF of the integrated pressure over the continuous area of a rectangular patch is the limit of that on discrete nodes of the rectangular patch when the number of nodes in each row or column goes to infinity. In Section 5, the closed-form formulas of the JAAF of the integrated pressure on rectangular patches, with estimated parameters of the model, are verified with the measurements of the uPSP and the conventional pressure transducer collected in the Space Launch System (SLS) Ascent Unsteady Aerodynamics Test (AUAT) at NASA Ames Research Center in November 2017. Finally, the conclusions are presented in Section 6.

The closed-form formulas of the JAAF of the integrated pressure on rectangular patches derived in this paper provide an efficient method to estimate the attenuation of integration by the decorrelation of the flow pressure field and set references for the comparison of the spectrum of the integrated uPSP measurements and the conventional pressure transducer measurements.

II. Model of the Surface Pressure Field

This section describes the model of the surface pressure field. It is assumed the aerodynamic surface pressure field is homogeneous. The PSD of the aerodynamic pressure at a point in the homogeneous surface pressure field, denoted as $\phi(f)$, is a function of the frequency f only and independent of the location of the point. The Cross Power Spectral Density (CPSD) of the pressure at two points in the homogeneous surface pressure field, denoted as $\phi_{CPSD}(\Delta x, \Delta y; f)$, is described with the Corcos model (Refs. [18]-[20]), as shown below

$$\phi_{CPSD}(\Delta x, \Delta y; f) = \phi(f) \cdot e^{-c_x k_c |\Delta x|} \cdot e^{-c_y k_c |\Delta y|} \cdot e^{-i k_c \Delta x} \quad (1)$$

In Eq. (1), Δx and Δy are components of the displacement between the two points along the streamline and across the streamline respectively, k_c is the convection wavenumber determined by the convection velocity U_c

$$k_c = 2\pi f / U_c \quad (2)$$

the coefficients c_x and c_y represent the decay of the surface pressure correlation in the directions along the streamline and across the streamline respectively, and i is the imaginary unit. It is noted that the CPSD of two points in the homogeneous surface pressure field is only related to the displacement of the two points and independent of their locations as well.

The Corcos model separates the dependence of the CPSD of the surface pressure in the directions along the streamline and across the streamline. As shown in the following sections, this feature simplifies the computation of the JAAF of the integrated pressure on rectangular patches, whose edges are defined in the direction along the streamline or across the streamline.

III. JAAF of Integrated Pressure on the Discrete Grid Nodes of a Rectangular Patch

In this section, it is assumed the measurements of the surface pressure field are only available on the discrete grid nodes of a rectangular patch and the JAAF of the integrated pressure on the rectangular patch is discussed. The edges of the rectangular patch are defined in the direction along the streamline or across the streamline. We start from the JAAF of the integrated pressure on a simple 3×3 two-dimensional array of discrete grid nodes of a rectangular patch, and then extend the results to the general case of the JAAF of the integrated pressure on an $m \times n$ two-dimensional array of discrete grid nodes of the rectangular patch.

Consider the integrated pressure on a 3×3 two-dimensional array of discrete grid nodes of a rectangular patch. As shown in Fig. 1, the 3 nodes in each of the 3 rows are evenly spaced along the streamline, and 3 nodes in each of the 3 columns are evenly spaced across the streamline. The distances between two neighbor nodes in the directions along the streamline and across the streamline are denoted as δ_x and δ_y , respectively. The arrow of the streamline shows the direction of the flow.

The integrated pressure on the 3×3 two-dimensional array of discrete grid nodes of the rectangular patch is determined as the mean of the pressure measurements on the $3 \cdot 3$ nodes. The PSD of the integrated pressure, denoted as $\phi_{PSD,3 \times 3}(f)$, is computed as

$$\phi_{PSD,3 \times 3}(f) = 1/(3 \cdot 3)^2 \cdot \sum_{element} \Phi_{CPSD,3 \times 3} \quad (3)$$

where $\Phi_{CPSD,3 \times 3}$ is the CPSD matrix of the pressure measurements on the 3×3 two-dimensional array of discrete grid nodes, as shown in the equation below, and $\sum_{element} \Phi_{CPSD,3 \times 3}$ is the sum of all elements of the CPSD matrix $\Phi_{CPSD,3 \times 3}$.

$$\Phi_{CPSD,3 \times 3} = \begin{bmatrix} \phi_{11,11} & \phi_{11,12} & \phi_{11,13} & | & \phi_{11,21} & \phi_{11,22} & \phi_{11,23} & | & \phi_{11,31} & \phi_{11,32} & \phi_{11,33} \\ \phi_{12,11} & \phi_{12,12} & \phi_{12,13} & | & \phi_{12,21} & \phi_{12,22} & \phi_{12,23} & | & \phi_{12,31} & \phi_{12,32} & \phi_{12,33} \\ \phi_{13,11} & \phi_{13,12} & \phi_{13,13} & | & \phi_{13,21} & \phi_{13,22} & \phi_{13,23} & | & \phi_{13,31} & \phi_{13,32} & \phi_{13,33} \\ - & - & - & | & - & - & - & | & - & - & - \\ \phi_{21,11} & \phi_{21,12} & \phi_{21,13} & | & \phi_{21,21} & \phi_{21,22} & \phi_{21,23} & | & \phi_{21,31} & \phi_{21,32} & \phi_{21,33} \\ \phi_{22,11} & \phi_{22,12} & \phi_{22,13} & | & \phi_{22,21} & \phi_{22,22} & \phi_{22,23} & | & \phi_{22,31} & \phi_{22,32} & \phi_{22,33} \\ \phi_{23,11} & \phi_{23,12} & \phi_{23,13} & | & \phi_{23,21} & \phi_{23,22} & \phi_{23,23} & | & \phi_{23,31} & \phi_{23,32} & \phi_{23,33} \\ - & - & - & | & - & - & - & | & - & - & - \\ \phi_{31,11} & \phi_{31,12} & \phi_{31,13} & | & \phi_{31,21} & \phi_{31,22} & \phi_{31,23} & | & \phi_{31,31} & \phi_{31,32} & \phi_{31,33} \\ \phi_{32,11} & \phi_{32,12} & \phi_{32,13} & | & \phi_{32,21} & \phi_{32,22} & \phi_{32,23} & | & \phi_{32,31} & \phi_{32,32} & \phi_{32,33} \\ \phi_{33,11} & \phi_{33,12} & \phi_{33,13} & | & \phi_{33,21} & \phi_{33,22} & \phi_{33,23} & | & \phi_{33,31} & \phi_{33,32} & \phi_{33,33} \end{bmatrix} \quad (4)$$

The element of the CPSD Matrix, $\phi_{i_1 j_1, i_2 j_2}$, is the CPSD of the pressure measurements on the nodes $i_1 j_1$ and $i_2 j_2$, where the row indices $i_1, i_2 = 1, 2, 3$, and the column indices $j_1, j_2 = 1, 2, 3$. Since the components of the displacement between the two nodes $i_1 j_1$ and $i_2 j_2$ along the streamline and across the streamline are $(j_2 - j_1)\delta_x$ and $(i_2 - i_1)\delta_y$ respectively, it is derived from Eq. (1) that

$$\phi_{i_1 j_1, i_2 j_2} = \phi(f) \cdot e^{-c_x k_c |j_2 - j_1| \delta_x} \cdot e^{-c_y k_c |i_2 - i_1| \delta_y} \cdot e^{-i k_c (j_2 - j_1) \delta_x} \quad (5)$$

Therefore, the CPSD matrix $\Phi_{CPSD,3 \times 3}$ in Eq. (4) can be rewritten in the following format

$$\Phi_{CPSD,3 \times 3} = \phi(f) \cdot \begin{bmatrix} \begin{bmatrix} 1 & z_x^1 & z_x^2 \\ \bar{z}_x^1 & 1 & z_x^1 \\ \bar{z}_x^2 & \bar{z}_x^1 & 1 \end{bmatrix} \cdot 1 & \begin{bmatrix} 1 & z_x^1 & z_x^2 \\ \bar{z}_x^1 & 1 & z_x^1 \\ \bar{z}_x^2 & \bar{z}_x^1 & 1 \end{bmatrix} \cdot z_y^1 & \begin{bmatrix} 1 & z_x^1 & z_x^2 \\ \bar{z}_x^1 & 1 & z_x^1 \\ \bar{z}_x^2 & \bar{z}_x^1 & 1 \end{bmatrix} \cdot z_y^2 \\ \begin{bmatrix} 1 & z_x^1 & z_x^2 \\ \bar{z}_x^1 & 1 & z_x^1 \\ \bar{z}_x^2 & \bar{z}_x^1 & 1 \end{bmatrix} \cdot z_y^1 & \begin{bmatrix} 1 & z_x^1 & z_x^2 \\ \bar{z}_x^1 & 1 & z_x^1 \\ \bar{z}_x^2 & \bar{z}_x^1 & 1 \end{bmatrix} \cdot 1 & \begin{bmatrix} 1 & z_x^1 & z_x^2 \\ \bar{z}_x^1 & 1 & z_x^1 \\ \bar{z}_x^2 & \bar{z}_x^1 & 1 \end{bmatrix} \cdot z_y^1 \\ \begin{bmatrix} 1 & z_x^1 & z_x^2 \\ \bar{z}_x^1 & 1 & z_x^1 \\ \bar{z}_x^2 & \bar{z}_x^1 & 1 \end{bmatrix} \cdot z_y^2 & \begin{bmatrix} 1 & z_x^1 & z_x^2 \\ \bar{z}_x^1 & 1 & z_x^1 \\ \bar{z}_x^2 & \bar{z}_x^1 & 1 \end{bmatrix} \cdot z_y^1 & \begin{bmatrix} 1 & z_x^1 & z_x^2 \\ \bar{z}_x^1 & 1 & z_x^1 \\ \bar{z}_x^2 & \bar{z}_x^1 & 1 \end{bmatrix} \cdot 1 \end{bmatrix} \quad (6)$$

where

$$z_x = e^{-c_x k_c \delta_x - i k_c \delta_x} \quad (7)$$

$$z_y = e^{-c_y k_c \delta_y} \quad (8)$$

\bar{z}_x is the conjugate of the complex number z_x .

The JAAF of the integrated pressure on the 3×3 two-dimensional array of discrete grid nodes of the rectangular patch, denoted as $J_{3 \times 3}(f)$, is defined as the ratio of the PSD of the integrated pressure on the $3 \cdot 3$ nodes, $\phi_{PSD,3 \times 3}(f)$, to the PSD of the pressure at a point, $\phi(f)$

$$J_{3 \times 3}(f) = \phi_{PSD,3 \times 3}(f) / \phi(f) \quad (9)$$

Since

$$\begin{aligned} \sum_{element} & \begin{bmatrix} \begin{bmatrix} 1 & z_x^1 & z_x^2 \\ \bar{z}_x^1 & 1 & z_x^1 \\ \bar{z}_x^2 & \bar{z}_x^1 & 1 \end{bmatrix} \cdot 1 & \begin{bmatrix} 1 & z_x^1 & z_x^2 \\ \bar{z}_x^1 & 1 & z_x^1 \\ \bar{z}_x^2 & \bar{z}_x^1 & 1 \end{bmatrix} \cdot z_y^1 & \begin{bmatrix} 1 & z_x^1 & z_x^2 \\ \bar{z}_x^1 & 1 & z_x^1 \\ \bar{z}_x^2 & \bar{z}_x^1 & 1 \end{bmatrix} \cdot z_y^2 \\ \begin{bmatrix} 1 & z_x^1 & z_x^2 \\ \bar{z}_x^1 & 1 & z_x^1 \\ \bar{z}_x^2 & \bar{z}_x^1 & 1 \end{bmatrix} \cdot z_y^1 & \begin{bmatrix} 1 & z_x^1 & z_x^2 \\ \bar{z}_x^1 & 1 & z_x^1 \\ \bar{z}_x^2 & \bar{z}_x^1 & 1 \end{bmatrix} \cdot 1 & \begin{bmatrix} 1 & z_x^1 & z_x^2 \\ \bar{z}_x^1 & 1 & z_x^1 \\ \bar{z}_x^2 & \bar{z}_x^1 & 1 \end{bmatrix} \cdot z_y^1 \\ \begin{bmatrix} 1 & z_x^1 & z_x^2 \\ \bar{z}_x^1 & 1 & z_x^1 \\ \bar{z}_x^2 & \bar{z}_x^1 & 1 \end{bmatrix} \cdot z_y^2 & \begin{bmatrix} 1 & z_x^1 & z_x^2 \\ \bar{z}_x^1 & 1 & z_x^1 \\ \bar{z}_x^2 & \bar{z}_x^1 & 1 \end{bmatrix} \cdot z_y^1 & \begin{bmatrix} 1 & z_x^1 & z_x^2 \\ \bar{z}_x^1 & 1 & z_x^1 \\ \bar{z}_x^2 & \bar{z}_x^1 & 1 \end{bmatrix} \cdot 1 \end{bmatrix} \\ & = \sum_{element} \begin{bmatrix} 1 & z_x^1 & z_x^2 \\ \bar{z}_x^1 & 1 & z_x^1 \\ \bar{z}_x^2 & \bar{z}_x^1 & 1 \end{bmatrix} \cdot \sum_{element} \begin{bmatrix} 1 & z_y^1 & z_y^2 \\ z_y^1 & 1 & z_y^1 \\ z_y^2 & z_y^1 & 1 \end{bmatrix} \end{aligned} \quad (10)$$

the JAAF of the integrated pressure on the 3×3 two-dimensional array of discrete grid nodes can be rewritten as

$$J_{3 \times 3}(f) = J_{x,3}(f) \cdot J_{y,3}(f) \quad (11)$$

where $J_{x,3}(f)$ and $J_{y,3}(f)$ are the JAAs in the directions along the streamline and across the streamline respectively, and

$$J_{x,3}(f) = 1/3^2 \cdot \sum_{element} \begin{bmatrix} 1 & z_x^1 & z_x^2 \\ \bar{z}_x^1 & 1 & z_x^1 \\ \bar{z}_x^2 & \bar{z}_x^1 & 1 \end{bmatrix} \quad (12)$$

$$J_{y,3}(f) = 1/3^2 \cdot \sum_{element} \begin{bmatrix} 1 & z_y^1 & z_y^2 \\ z_y^1 & 1 & z_y^1 \\ z_y^2 & z_y^1 & 1 \end{bmatrix} \quad (13)$$

Eq. (11) shows the JAAF of the integrated pressure on the rectangular patch is equal to the product of the JAAFs in the directions along the streamline and across the streamline, which is based on the Corcos model that separates the dependence of the CPSD of the surface pressure in the directions along the streamline and across the streamline.

Eq. (13) can be simplified as

$$\begin{aligned} J_{y,3}(f) &= \frac{1}{3^2} \cdot \sum_{element} \begin{bmatrix} 1 & z_y^1 & z_y^2 \\ z_y^1 & 1 & z_y^1 \\ z_y^2 & z_y^1 & 1 \end{bmatrix} = \frac{1}{3^2} \cdot \left\{ 2 \cdot \sum_{element} \begin{bmatrix} 1 & z_y^1 & z_y^2 \\ 0 & 1 & z_y^1 \\ 0 & 0 & 1 \end{bmatrix} - 3 \right\} \\ &= \frac{1}{3^2} \cdot \left\{ 2 \cdot \left[\frac{1-z_y^3}{1-z_y} + \frac{1-z_y^2}{1-z_y} + \frac{1-z_y^1}{1-z_y} \right] - 3 \right\} = \frac{1}{3^2} \cdot \left\{ 2 \cdot \left[\frac{3}{1-z_y} - z_y \cdot \frac{1-z_y^3}{(1-z_y)^2} \right] - 3 \right\} \\ &= 2 \cdot \left[\frac{1}{3 \cdot (1-z_y)} - z_y \cdot \frac{1-z_y^3}{3^2 \cdot (1-z_y)^2} \right] - \frac{1}{3} \end{aligned} \quad (14)$$

Since the sum of a complex number z and its conjugate \bar{z} is equal to the sum of $Re(z)$ and $Re(\bar{z})$, where $Re(z)$ is the real part of z , Eq. (12) can be simplified as following

$$\begin{aligned} J_{x,3}(f) &= \frac{1}{3^2} \cdot \sum_{element} \begin{bmatrix} 1 & z_x^1 & z_x^2 \\ \bar{z}_x^1 & 1 & z_x^1 \\ \bar{z}_x^2 & \bar{z}_x^1 & 1 \end{bmatrix} = \frac{1}{3^2} \cdot Re \left\{ \sum_{element} \begin{bmatrix} 1 & z_x^1 & z_x^2 \\ z_x^1 & 1 & z_x^1 \\ z_x^2 & z_x^1 & 1 \end{bmatrix} \right\} \\ &= \frac{1}{3^2} \cdot Re \left\{ 2 \cdot \sum_{element} \begin{bmatrix} 1 & z_x^1 & z_x^2 \\ 0 & 1 & z_x^1 \\ 0 & 0 & 1 \end{bmatrix} - 3 \right\} \\ &= \frac{1}{3^2} \cdot Re \left\{ 2 \cdot \left[\frac{1-z_x^3}{1-z_x} + \frac{1-z_x^2}{1-z_x} + \frac{1-z_x^1}{1-z_x} \right] - 3 \right\} = \frac{1}{3^2} \cdot Re \left\{ 2 \cdot \left[\frac{3}{1-z_x} - z_x \cdot \frac{1-z_x^3}{(1-z_x)^2} \right] - 3 \right\} \\ &= 2 \cdot Re \left[\frac{1}{3 \cdot (1-z_x)} - z_x \cdot \frac{1-z_x^3}{3^2 \cdot (1-z_x)^2} \right] - \frac{1}{3} \end{aligned} \quad (15)$$

Eqs. (7), (8), (11), (14) and (15) provide the closed-form formulas to compute the JAAF of the integrated pressure on the 3×3 two-dimensional array of discrete grid nodes of a rectangular patch.

The closed-form formulas of the JAAF of the integrated pressure on the 3×3 two-dimensional array of discrete grid nodes of a rectangular patch, as shown in Fig. 1, can be extended to the general case of the JAAF of the integrated pressure on an $m \times n$ two-dimensional array of discrete grid nodes of a rectangular patch. As shown in Fig. 2, the n nodes in each of the m rows are evenly spaced along the streamline, and m nodes in each of the n columns are evenly spaced across the streamline. The distances between two neighbor nodes in the directions along the streamline and across the streamline are also denoted as δ_x and δ_y respectively.

The integrated pressure on the $m \times n$ two-dimensional array of discrete grid nodes of the rectangular patch is determined as the mean of the pressure measurements on the $m \cdot n$ nodes. The PSD of the integrated pressure, denoted as $\phi_{PSD,m \times n}(f)$, is computed as

$$\phi_{PSD,m \times n}(f) = 1/(m \cdot n)^2 \cdot \sum_{element} \Phi_{CPSD,m \times n} \quad (16)$$

where $\Phi_{CPSD,m \times n}$ is the CPSD matrix of the pressure measurements on the $m \times n$ two-dimensional array of discrete grid nodes, and

$$\Phi_{CPSD,m \times n} = \begin{bmatrix} \phi_{11,11} & \dots & \phi_{11,mn} \\ \dots & \dots & \dots \\ \phi_{mn,11} & \dots & \phi_{mn,mn} \end{bmatrix} \quad (17)$$

The element of the CPSD matrix, $\phi_{i_1 j_1, i_2 j_2}$, is the CPSD of the pressure measurements on the nodes $i_1 j_1$ and $i_2 j_2$, where the row indices $i_1, i_2 = 1, \dots, m$, and the column indices $j_1, j_2 = 1, \dots, n$. Eq. (5) is also true for the $m \times n$ two-dimensional array of discrete grid nodes.

The JAAF of the integrated pressure on the $m \times n$ two-dimensional array of discrete grid nodes of the rectangular patch, denoted as $J_{m \times n}(f)$, is defined as the ratio of the PSD of integrated pressure on the $m \cdot n$ nodes, $\phi_{PSD,m \times n}(f)$, to the PSD of the pressure at a point, $\phi(f)$

$$J_{m \times n}(f) = \phi_{PSD,m \times n}(f) / \phi(f) \quad (18)$$

Similar to Eq. (11), we have

$$J_{m \times n}(f) = J_{x,n}(f) \cdot J_{y,m}(f) \quad (19)$$

where $J_{x,n}(f)$ and $J_{y,m}(f)$ are JAAs in the directions along the streamline and across the streamline respectively, and

$$J_{x,n}(f) = \frac{1}{n^2} \cdot \sum_{element} \begin{bmatrix} 1 & z_x^1 & \dots & z_x^{n-2} & z_x^{n-1} \\ \bar{z}_x^1 & 1 & \dots & z_x^{n-3} & z_x^{n-2} \\ \dots & \dots & \dots & \dots & \dots \\ \bar{z}_x^{n-2} & \bar{z}_x^{n-3} & \dots & 1 & z_x^1 \\ \bar{z}_x^{n-1} & \bar{z}_x^{n-2} & \dots & \bar{z}_x^1 & 1 \end{bmatrix} = 2 \cdot Re \left[\frac{1}{n \cdot (1-z_x)} - z_x \cdot \frac{1-z_x^n}{n^2 \cdot (1-z_x)^2} \right] - \frac{1}{n} \quad (20)$$

$$J_{y,m}(f) = \frac{1}{m^2} \cdot \sum_{element} \begin{bmatrix} 1 & z_y^1 & \dots & z_y^{m-2} & z_y^{m-1} \\ z_y^1 & 1 & \dots & z_y^{m-3} & z_y^{m-2} \\ \dots & \dots & \dots & \dots & \dots \\ z_y^{m-2} & z_y^{m-3} & \dots & 1 & z_y^1 \\ z_y^{m-1} & z_y^{m-2} & \dots & z_y^1 & 1 \end{bmatrix} = 2 \cdot \left[\frac{1}{m \cdot (1-z_y)} - z_y \cdot \frac{1-z_y^m}{m^2 \cdot (1-z_y)^2} \right] - \frac{1}{m} \quad (21)$$

Eqs. (7), (8), (19), (20) and (21) provide the closed-form formulas to compute the JAAF of the integrated pressure on the $m \times n$ two-dimensional array of discrete grid nodes of a rectangular patch.

IV. JAAF of Integrated Pressure over the Continuous Area of a Rectangular Patch

In this section, we assume the measurements of the surface pressure field are available over the continuous area of a rectangular patch and discuss the JAAF of the integrated pressure on the rectangular patch. As shown in Fig. 3, the edges of the rectangle patch are in the directions along the streamline and across the streamline, and the length and width are labelled as L and W respectively.

The integrated pressure over the continuous area of the rectangular patch is determined as the surface integral of the pressure measurements over the rectangular patch, divided by the area of the rectangular patch. The PSD of the integrated pressure, denoted as $\phi_{PSD,L \times W}(f)$, is computed as

$$\phi_{PSD,L \times W}(f) = \frac{1}{(L \cdot W)^2} \cdot \int_{-W/2}^{+W/2} \int_{-L/2}^{+L/2} \int_{-W/2}^{+W/2} \int_{-L/2}^{+L/2} \phi_{CPSD}(x_2 - x_1, y_2 - y_1; f) dx_1 dy_1 dx_2 dy_2 \quad (22)$$

The JAAF of the integrated pressure on the rectangular patch, denoted as $J_{L \times W}(f)$, is defined as the ratio of the PSD of integrated pressure on the rectangular patch, $\phi_{PSD, L \times W}(f)$, to the PSD of the pressure at a point of the patch, $\phi(f)$

$$J_{L \times W}(f) = \phi_{PSD, L \times W}(f) / \phi(f) \quad (23)$$

Combining Eqs. (1) and (23) leads to

$$J_{L \times W}(f) = 1/(L \cdot W)^2 \cdot \int_{-W/2}^{+W/2} \int_{-L/2}^{+L/2} \int_{-W/2}^{+W/2} \int_{-L/2}^{+L/2} e^{-c_x k_c |x_2 - x_1|} \cdot e^{-c_y k_c |y_2 - y_1|} \cdot e^{-ik_c(x_2 - x_1)} dx_1 dy_1 dx_2 dy_2 \quad (24)$$

Similar to Eqs. (11) and (19), we have

$$J_{L \times W}(f) = J_{x,L}(f) \cdot J_{y,W}(f) \quad (25)$$

where $J_{x,L}(f)$ and $J_{y,W}(f)$ are JAAFs in the directions along the streamline and across the streamline respectively, and

$$J_{x,L}(f) = 1/L^2 \cdot \int_{-L/2}^{+L/2} \int_{-L/2}^{+L/2} e^{-c_x k_c |x_2 - x_1|} \cdot e^{-ik_c(x_2 - x_1)} dx_1 dx_2 \quad (26)$$

$$J_{y,W}(f) = 1/W^2 \cdot \int_{-W/2}^{+W/2} \int_{-W/2}^{+W/2} e^{-c_y k_c |y_2 - y_1|} dy_1 dy_2 \quad (27)$$

By definition, $J_{L \times W}(f)$ is computed with the multiple integral of 4 variables, as shown in Eq. (24). Eq. (25) shows that $J_{L \times W}(f)$ is equal to the product of $J_{x,L}(f)$ and $J_{y,W}(f)$, each of which is computed with a double integral of 2 variables, as shown in Eqs. (26) and (27). The simplification in the computation of $J_{L \times W}(f)$ is based on the separation of variables in the directions along the streamline and across the streamline, which again is based on the separation of dependence of the CPSD of the surface pressure in the Corcos model.

Eqs. (26) and (27) can be simplified as following

$$\begin{aligned} J_{x,L}(f) &= 1/L^2 \cdot \int_{-L/2}^{+L/2} \int_{-L/2}^{+L/2} e^{-c_x k_c |x_2 - x_1|} \cdot e^{-ik_c(x_2 - x_1)} dx_1 dx_2 \\ &= 1/L^2 \cdot \int_{-L/2}^{+L/2} dx_1 \int_{-L/2}^{x_1} e^{-c_x k_c(x_1 - x_2)} \cdot e^{-ik_c(x_2 - x_1)} dx_2 + 1/L^2 \cdot \int_{-L/2}^{+L/2} dx_1 \int_{x_1}^{+L/2} e^{-c_x k_c(x_2 - x_1)} \cdot e^{-ik_c(x_2 - x_1)} dx_2 \\ &= 1/L^2 \cdot \int_{-L/2}^{+L/2} e^{-c_x k_c x_1 + ik_c x_1} dx_1 \int_{-L/2}^{x_1} e^{c_x k_c x_2 - ik_c x_2} dx_2 + 1/L^2 \cdot \int_{-L/2}^{+L/2} e^{c_x k_c x_1 + ik_c x_1} dx_1 \int_{x_1}^{+L/2} e^{-c_x k_c x_2 - ik_c x_2} dx_2 \\ &= \frac{2c_x}{(c_x^2 + 1) \cdot k_c L} - \frac{2(c_x^2 - 1)[1 - e^{-c_x k_c L} \cos(k_c L)] + 4c_x e^{-c_x k_c L} \sin(k_c L)}{(c_x^2 + 1)^2 \cdot (k_c L)^2} \end{aligned} \quad (28)$$

$$\begin{aligned} J_{y,W}(f) &= 1/W^2 \cdot \int_{-W/2}^{+W/2} \int_{-W/2}^{+W/2} e^{-c_y k_c |y_2 - y_1|} dy_1 dy_2 \\ &= 1/W^2 \cdot \int_{-W/2}^{+W/2} dy_1 \int_{-W/2}^{y_1} e^{-c_y k_c(y_1 - y_2)} dy_2 + 1/W^2 \cdot \int_{-W/2}^{+W/2} dy_1 \int_{y_1}^{+W/2} e^{-c_y k_c(y_2 - y_1)} dy_2 \\ &= 1/W^2 \cdot \int_{-W/2}^{+W/2} e^{-c_y k_c y_1} dy_1 \int_{-W/2}^{y_1} e^{c_y k_c y_2} dy_2 + 1/W^2 \cdot \int_{-W/2}^{+W/2} e^{c_y k_c y_1} dy_1 \int_{y_1}^{+W/2} e^{-c_y k_c y_2} dy_2 \\ &= \frac{2}{c_y \cdot k_c W} - \frac{2(1 - e^{-c_y k_c W})}{c_y^2 \cdot (k_c W)^2} \end{aligned} \quad (29)$$

Eqs. (25), (28) and (29) provide the closed-form formulas of the JAAF of the integrated pressure on the continuous area of a rectangular patch.

Next, we will show that Eqs. (28) and (29) can also be derived as the limit cases of Eqs. (20) and (21) when the number of discrete grid nodes in each row and column of the two-dimensional array goes to infinity. As shown in Fig. 4, it is assumed the rectangular patch with length L and width W is covered with an $m \times n$ two-dimensional array of discrete grid nodes. Therefore, the distances between two neighbor nodes in the directions along the streamline and across the streamline, denoted as δ_x and δ_y respectively, are determined as

$$\delta_x = L/n \quad (30)$$

$$\delta_y = W/m \quad (31)$$

When the integers n and m go to infinity, δ_x and δ_y will go to zero. Based on the definitions of z_x and z_y given in Eqs. (7) and (8), we have

$$\lim_{n \rightarrow \infty} z_x = \lim_{\delta_x \rightarrow 0} e^{-(c_x+i)k_c \delta_x} = 1 \quad (32)$$

$$\lim_{m \rightarrow \infty} z_y = \lim_{\delta_y \rightarrow 0} e^{-c_y k_c \delta_y} = 1 \quad (33)$$

$$\lim_{n \rightarrow \infty} z_x^n = \lim_{n \rightarrow \infty} e^{-(c_x+i)k_c \frac{L}{n} n} = e^{-(c_x+i)k_c L} \quad (34)$$

$$\lim_{m \rightarrow \infty} z_y^m = \lim_{m \rightarrow \infty} e^{-c_y k_c \frac{W}{m} m} = e^{-c_y k_c W} \quad (35)$$

$$\lim_{n \rightarrow \infty} n(1 - z_x) = \lim_{n \rightarrow \infty} n[1 - e^{-(c_x+i)k_c \frac{L}{n}}] = (c_x + i)k_c L \quad (36)$$

$$\lim_{m \rightarrow \infty} m(1 - z_y) = \lim_{m \rightarrow \infty} m(1 - e^{-c_y k_c \frac{W}{m}}) = c_y k_c W \quad (37)$$

$J_{x,L}(f)$ and $J_{y,W}(f)$ can be determined as the limits of $J_{x,n}(f)$ and $J_{y,m}(f)$ given in Eqs. (20) and (21), when the integers n and m go to infinity respectively,

$$\begin{aligned} J_{x,L}(f) &= \lim_{n \rightarrow \infty} J_{x,n}(f) = \lim_{n \rightarrow \infty} \left\{ 2 \cdot \operatorname{Re} \left[\frac{1}{n \cdot (1 - z_x)} - z_x \cdot \frac{1 - z_x^n}{n^2 \cdot (1 - z_x)^2} \right] - \frac{1}{n} \right\} \\ &= 2 \cdot \operatorname{Re} \left[\frac{1}{(c_x+i) \cdot k_c L} - \frac{1 - e^{-(c_x+i)k_c L}}{(c_x+i)^2 \cdot (k_c L)^2} \right] \\ &= \frac{2c_x}{(c_x^2+1) \cdot k_c L} - \frac{2(c_x^2-1)[1 - e^{-c_x k_c L} \cos(k_c L)] + 4c_x e^{-c_x k_c L} \sin(k_c L)}{(c_x^2+1)^2 \cdot (k_c L)^2} \end{aligned} \quad (38)$$

$$\begin{aligned} J_{y,W}(f) &= \lim_{m \rightarrow \infty} J_{y,m}(f) = \lim_{m \rightarrow \infty} \left\{ 2 \cdot \left[\frac{1}{m \cdot (1 - z_y)} - z_y \cdot \frac{1 - z_y^m}{m^2 \cdot (1 - z_y)^2} \right] - \frac{1}{m} \right\} \\ &= \frac{2}{c_y \cdot k_c W} - \frac{2(1 - e^{-c_y k_c W})}{c_y^2 \cdot (k_c W)^2} \end{aligned} \quad (39)$$

As expected, Eqs. (38) and (39) are consistent with Eqs. (28) and (29) respectively. Therefore, it is shown that the JAAF of the integrated pressure on the continuous area of a rectangular patch is the limit of the JAAF of the integrated pressure on the discrete grid nodes of the rectangular patch when the number of nodes in each row and column go to infinity.

V. Verification of the JAAF with the SLS AUAT Data

In this section, the closed-form formulas of the JAAF of the integrated pressure on rectangular patches derived in the previous sections, with estimated parameters of the Corcos model, are verified with the measurements of the uPSP and the conventional pressure transducer of the SLS AUAT. Fig. 5 shows the SLS Block 1B crew scale model, with the uPSP applied to the model surface, in the 11-by-11-foot transonic test section of the Unitary Plan Wind Tunnel (UPWT) at NASA Ames Research Center from a test conducted in November 2017. The uPSP measurements were collected with four Phantom v2512 high-speed cameras at 10,000 frames per second and processed with the uPSP data processing software (Ref. [21-23]).

Three rectangular patches, labeled as Patches #1, #2 and #3 respectively, are defined on the Universal Stage Adapter (USA) component of the scale model. As shown in Fig. 6, Patches #1, #2, and #3 are illustrated as rectangles in green, blue, and red respectively, whose edges are in the direction along the streamline or across the streamline. The patches are covered with evenly spaced two-dimensional grid nodes. The distances between the two neighbor nodes, δ_x and δ_y , are both approximately 0.1 inch. There are 150 grid nodes in Patch #1 and 300 grid nodes in Patches #2 and #3. The black dot in Fig. 6 indicates a conventional pressure transducer, a Kulite labeled as KA907. Note that the three rectangular patches are defined intentionally not to cover the Kulite, since there are no valid uPSP measurements available in the region of the Kulite (Ref. [10]).

Fig. 7 shows the JAAF of the integrated pressure on the three rectangular patches of a SLS AUAT configuration, computed with the closed-form formulas. In the SLS AUAT configuration, the freestream Mach number is 0.95 and the angle of attack and the angle of sideslip, denoted as α and β respectively, are both 0.0 degree. The following parameters of the Corcos model are estimated with the measurements of uPSP and conventional pressure transducers in the defined patch area: the convection velocity $U_c = 5,316$ inch/second, and the coefficients $c_x = 0.1$, $c_y = 0.7$. Compared to Patch #1, Patches #2 and #3 extend in the directions along the streamline and across the streamline respectively. The corresponding decorrelation of the flow pressure field, both streamwise and spanwise, can be observed in the variations of the JAAFs of the integrated pressure on Patches #2 and #3 (in blue and red respectively) from the JAAF of the integrated pressure on Patch #1 (in green), as shown in Fig. 7.

Fig. 8 shows the PSD of the integrated pressure of the uPSP measurements and the estimated PSD of the integrated pressure on Patches #1, #2 and #3, in the subplots (a), (b) and (c) respectively, of the same SLS AUAT configuration as that of Fig. 7. The PSDs of the integrated pressure of the uPSP measurements on Patches #1, #2 and #3 are illustrated as thin lines in light green, light blue and magenta respectively. As a reference, the PSD of the measurement of Kulite KA907 is also illustrated as the thick line in black. Please note the estimated levels of the shot noise are removed from the PSD of the integrated pressure of the uPSP measurements on the patches, and a constant is applied to the PSD of the Kulite measurement to compensate the difference in the scale factors of the uPSP and Kulite. The estimated PSDs of the integrated pressure on Patches #1, #2, and #3, which are illustrated as thick lines in green, blue, and red respectively, are determined as the product of the compensated PSD of the Kulite measurement and the computed JAAF of the integrated pressure on the corresponding patch. It is observed the estimated PSD of the integrated pressure on the rectangular patch is consistent with the PSD of the integrated pressure of the uPSP measurements on the corresponding patch, which verifies the closed-form formulas of the JAAF of the integrated pressure on rectangular patches.

VI. Conclusions

This paper discusses the JAAF of the integrated pressure with uPSP measurements. The JAAF, a function of frequency, is defined as the ratio of the PSD of the integrated aerodynamic pressure on the patch to the average PSD of the aerodynamic pressure on the grid nodes of the patch. The JAAF is investigated for the integrated pressure on rectangular patches, whose edges are defined in the direction along the streamline or across the streamline. Based on the assumption that the surface pressure field can be described by the Corcos model, the closed-form formulas to compute the JAAF of the integrated pressure on the discrete grid nodes of a rectangular patch and over the continuous area of a rectangular patch are derived respectively. It is shown that the JAAF of the integrated pressure over the continuous area of a rectangular patch is the limit of that on discrete nodes of the rectangular patch when the number of nodes in each row or column goes to infinity. In the paper, the closed-form formulas of the JAAF of the integrated

pressure on rectangular patches, with estimated parameters of the Corcos model, are verified with the measurements of the uPSP and the conventional pressure transducer collected in the SLS AUAT at NASA Ames Research Center in November 2017.

The closed-form formulas of the JAAF of the integrated pressure on rectangular patches, which are based on the Corcos model, provide an efficient method to estimate the attenuation of integration by the decorrelation of the flow pressure field. The methodology of this paper can be extended to derive the closed-form formulas of the JAAF of the CPSD of integrated pressures on two non-overlapped or overlapped rectangular patches. The results set references for the comparison of the spectrum of the integrated uPSP measurements and the conventional pressure transducer measurements.

Acknowledgment

The work described in this paper is a part of NASA's development of a new state-of-the-art uPSP capability in production wind tunnels. Funding was provided by the NASA Aerosciences Evaluation and Test Capabilities (AETC) Portfolio Office. The authors would like to thank Jennifer Baerny, Christopher Barreras, James Bell, Nicholas Califano, Ross Flach, Lawrence Hand, Patrick Heaney, Jaffar Iqbal, Kenji Kato, Alan Landman, Bruce Laverde, Kenneth Lyons, Blair Mclachlan, Jack Ortega, Jayanta Panda, David Piatak, Victoria Pollard, James Ramey, Martin Sekula, Francesco Soranna, Thomas Steva, Paul Stremel and Thomas Volden for their expertise and advice for the research work of this paper.

References

- [1] Bell, J. H., Schairer, E. T., Hand, L. A., and Mehta, R.D., "Surface Pressure Measurements Using Luminescent Coatings", *Annual Review of Fluid Mechanics*, Vol. 33, No. 1, 2001, pp. 155-206.
- [2] Liu, T. and Sullivan, J. P., *Pressure and Temperature Sensitive Paints*, Springer-Verlag, 2005.
- [3] Gregory, J. W., Asai, K., Kameda, M., Liu, T., and Sullivan, J. P., "A Review of Pressure-Sensitive Paint for High-Speed and Unsteady Aerodynamics", *Proceedings of the Institution of Mechanical Engineers, Part G, Journal of Aerospace Engineering*, Vol. 222, No. 2, 2008, pp. 249-290.
- [4] Gregory, J. W., Sakaue, H., Liu, T., and Sullivan, J. P., "Fast Pressure-Sensitive Paint for Flow and Acoustic Diagnostics", *Annual Review of Fluid Mechanics*, Vol. 46, 2014, pp. 303-330.
- [5] Sellers, M. E., Nelson, M. A., and Crafton, J.W., "Dynamic Pressure-Sensitive Paint Demonstration in the AEDC Propulsion Wind Tunnel 16T", AIAA Paper 2016-1146, 54th AIAA Aerospace Sciences Meeting, San Diego, CA, January 2016.
- [6] Schuster, D. M., Panda, J., Ross, J. C., Roozeboom, N. H., Burnside, N., Ngo, C. L., Kumagai, H., Sellers, M. E., Powell, J. M., Sekula, M. K., and Piatak, D. J., "Investigation of Unsteady Pressure-Sensitive Paint (uPSP) and a Dynamic Loads Balance to Predict Launch Vehicle Buffet Environments", NASA Engineering and Safety Center Report TI-14-00962, 2016.
- [7] Sellers, M. E., Nelson, M. A., Roozeboom, N. H., and Burnside, N. J., "Evaluation of Unsteady Pressure Sensitive Paint Measurement Technique for Space Launch Vehicle Buffet Determination", AIAA Paper 2017-1402, 55th AIAA Aerospace Sciences Meeting, Grapevine, TX, January 2017.
- [8] Roozeboom, N. H., Ngo, C. L., Powell, J. M., Murakami, D. D., Ross, J. C., Murman, S. M., and Baerny, J. K., "Data Processing Methods for Unsteady Pressure-Sensitive Paint Application", AIAA 2018-1031, 56th AIAA Aerospace Sciences Meeting, Kissimmee, Florida, January 2018.
- [9] Roozeboom, N. H., Powell, J. M., Baerny, J. K., Murakami, D. D., Ngo, C. L., Garbeff, T. J., Ross, J. C., and Flach, R. L., "Development of Unsteady Pressure-Sensitive Paint Application on NASA Space Launch System", AIAA Paper 2019-3502, AIAA Aviation Forum, Dallas, TX, June 2019.
- [10] Roozeboom, N. H., Murakami, D. D., Li, J., Powell, J. M., Baerny, J. K., Stremel, P. M., Volden, T. R., Flach, R. L., Douthitt, A. N., Steva, T. B., Ross, J. C., and Bell, J. H., "Recent Developments in NASA's Unsteady Pressure-Sensitive Paint Capability", AIAA Paper 2020-0516, AIAA SciTech Forum, Orlando, FL, January 2020.

- [11] Roozeboom, N. H., Diosady, L. T., Murman, S. M., Burnside, N. J., Panda, J., and Ross, J. C., “Unsteady PSP Measurements on a Flat Plate Subject to Vortex Shedding from a Rectangular Prism”, AIAA Paper 2016-2017, 54th AIAA Aerospace Sciences Meeting, San Diego, CA, January 2016.
- [12] Panda, J., “Experimental Verification of Buffet Calculation Procedure Using Unsteady Pressure-Sensitive Paint”, *Journal of Aircraft*, Vol.54, No. 5, 2017, pp. 1791-1801.
- [13] Panda, J., Roozeboom, N.H., and Ross, J. C., “Wavenumber-Frequency Spectra on a Launch Vehicle Model Measured via Unsteady Pressure-Sensitive Paint”, *AIAA Journal*, Vol. 57, No. 5, 2019, pp. 1801-1817.
- [14] Tang, L., Hand, L., Murakami, Roozeboom, N., and Shaw-Lecerf, M., “Unsteady Pressure-Sensitive Paint Shot Noise Reduction”, AIAA Paper 2021-2579, AIAA Aviation Forum, Virtual Event, August 2021.
- [15] Powell, A., “On the Fatigue Failure of Structures due to Vibrations Excited by Random Pressure Fields”, *The Journal of the Acoustical Society of America*, Vol. 30, No. 12, 1958, pp. 1130-1135.
- [16] Bremner, P., “Two Factor Calibration of uPSP Wind Tunnel Data”, AeroHydroPLUS Technical Memorandum (internal document), December 2021.
- [17] Bremner, P., Shaw-Lecerf, M., Roozeboom, N. and Li, J., “Noise Reduction and Calibration of Unsteady Pressure-Sensitive Paint for High Resolution Measurement of Aero-acoustic Loads”, Spacecraft and Launch Vehicle Dynamic Environments Workshop, Virtual Event, June 2022.
- [18] Corcos, G.M., “Resolution of Pressure in Turbulence”, *The Journal of the Acoustical Society of America*, Vol.35, No.2, 1963, pp.192-199.
- [19] Bremner, P.G. and Wilby, J.F., “Aero-Vibro-Acoustics: Problem Statement and Methods for Simulation-Based Design Solution”, AIAA Paper 2002-2551, 8th AIAA/CEAS Aeroacoustics Conference, Breckenridge, CO, June 2002.
- [20] Soranna, F., Heaney, P.S., Sekula, M.K., Piatak, D.J., and Ramey, J.M., “Validation of the Corcos Model for the Space Launch System using Unsteady Pressure Sensitive Paint”, AIAA Paper 2022-3445, AIAA Aviation Forum, Chicago, IL & Virtual, June 2022.
- [21] Powell, J. M., Murman, S. M., Ngo, C. L., Roozeboom, N. H., Murakami, D. D., Baerny, J. K., and Li, J., “Development of Unsteady-PSP Data Processing and Analysis Tools for the NASA Ames Unitary 11ft Wind Tunnel”, AIAA Paper 2020-0292, AIAA SciTech Forum, Orlando, FL, January 2020.
- [22] Roozeboom, N., Murakami, D., Li, J., Shaw-Lecerf, M., Lash, E.L., Califano, N., Stremel, P., Lyons, K., Baerny, J., Barreras, C., Ortega, J., Kato, K., Hand, L. and McLachlan, B., “NASA’s Unsteady Pressure-Sensitive Paint Research and Operational Capability Developments”, AIAA SciTech Forum, National Harbor, MD & Virtual, January 2023.
- [23] Shaw-Lecerf, M., Lash, E.L., Murakami, D., Roozeboom, N., Li, J. and Bremner, P., “Methodology for Validation of Unsteady Pressure-Sensitive Paint Measurements using Pressure Transducers”, AIAA SciTech Forum, National Harbor, MD & Virtual, January 2023.

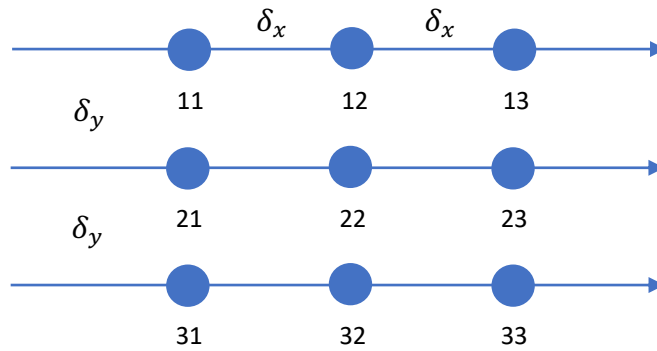


Fig. 1 A 3×3 two-dimensional array of discrete grid nodes of a rectangular patch

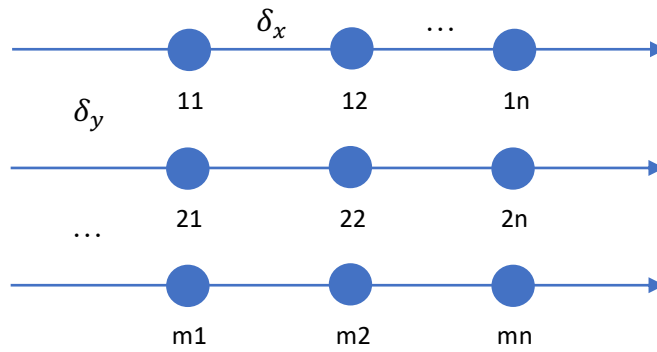


Fig. 2 An $m \times n$ two-dimensional array of discrete grid nodes of a rectangular patch

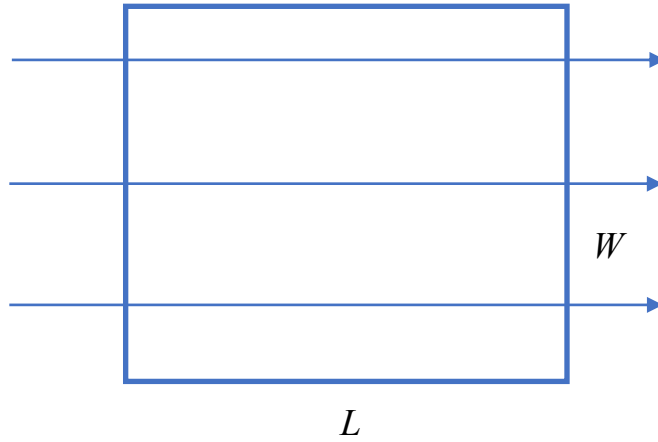


Fig. 3 A rectangular patch with length L and width W

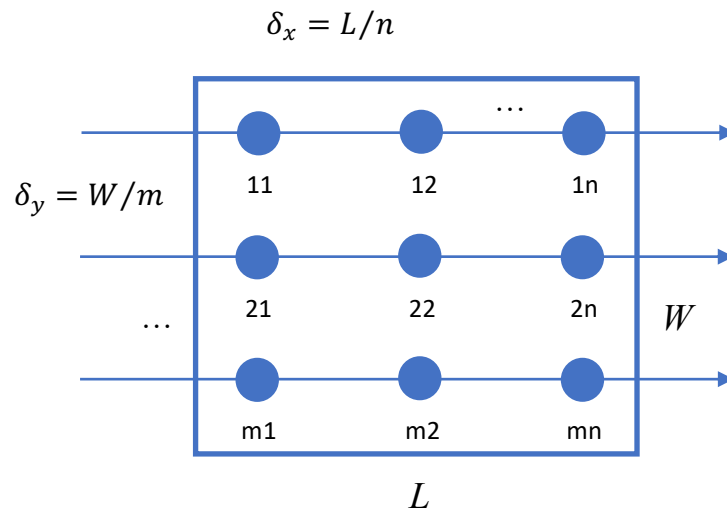


Fig. 4 A rectangular patch with length L and width W , covered with an $m \times n$ two-dimensional array of discrete grid nodes

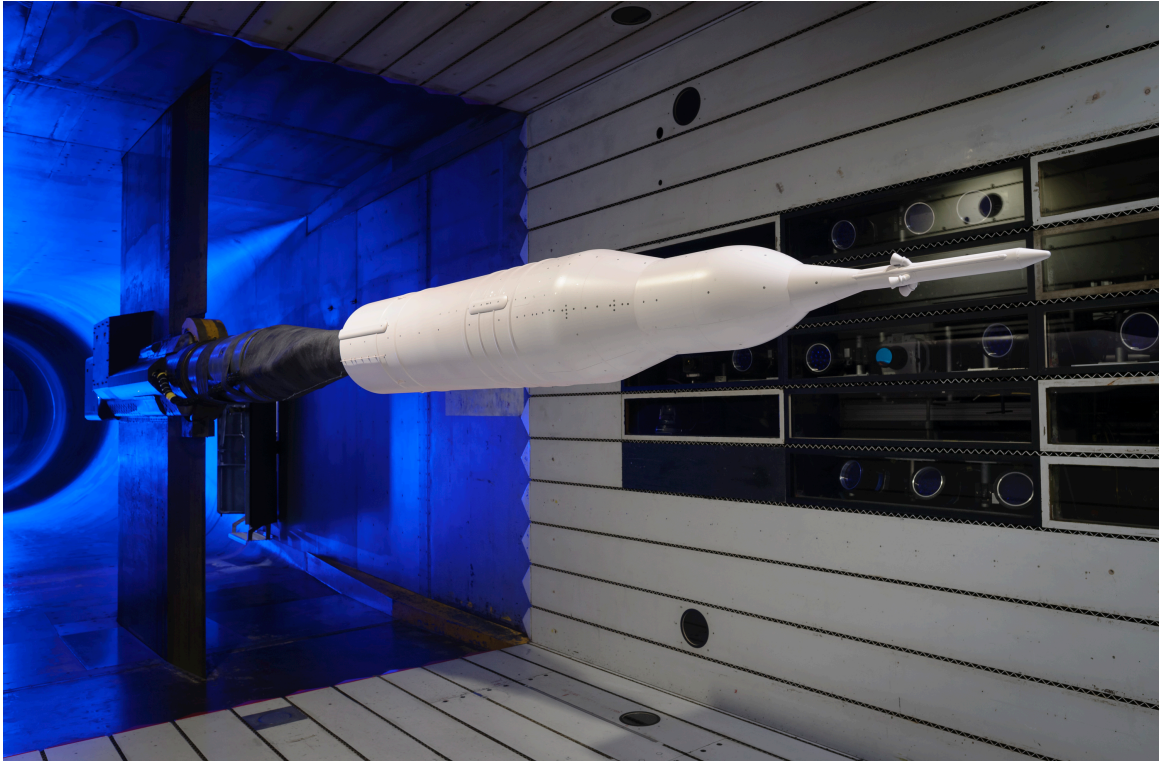


Fig. 5 SLS Block 1B scale model with uPSP in the 11-by-11-foot transonic test section of the UPWT at NASA Ames Research Center during the AUAT

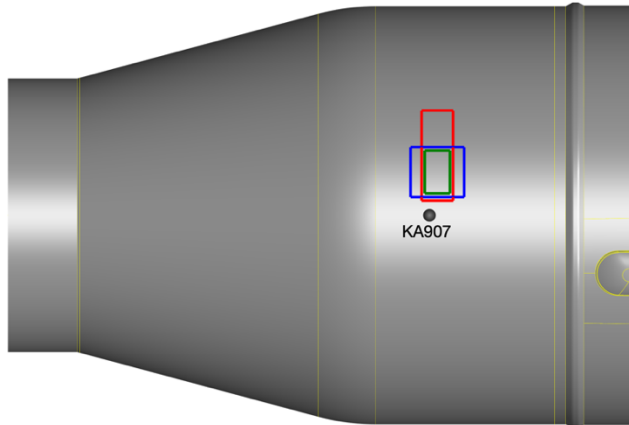


Fig. 6 Rectangular patches #1, #2 and #3 on the USA component of the model, illustrated as rectangles in green, blue and red respectively. The black dot indicates a conventional pressure transducer, a Kulite labeled as KA907.

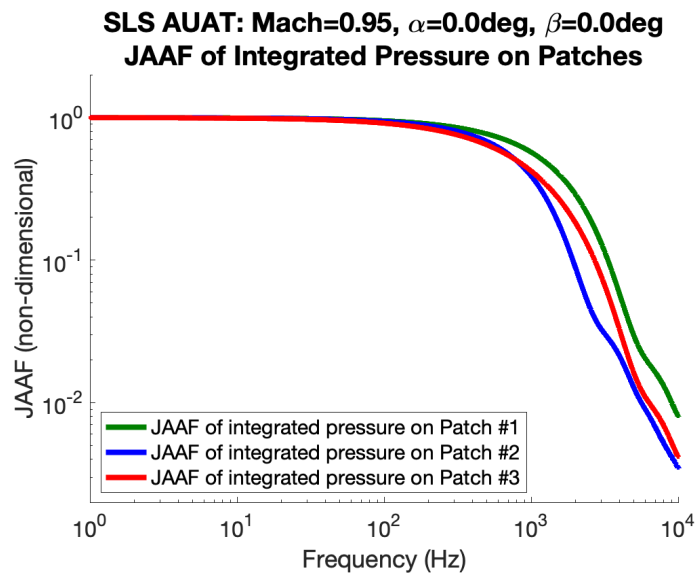
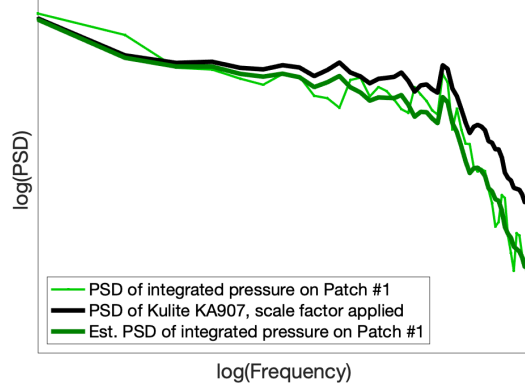


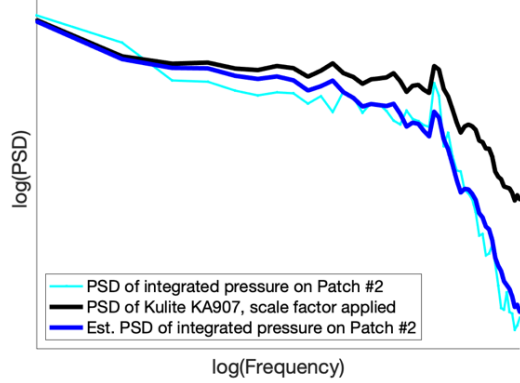
Fig. 7 JAAF of integrated pressure on Patches #1, #2 and #3 of the SLS AUAT configuration with Mach number 0.95, angle of attack 0.0 degree and angle of sideslip 0.0 degree

**SLS AUAT: Mach=0.95, $\alpha=0.0\text{deg}$, $\beta=0.0\text{deg}$
PSD and Est. PSD of Integrated Pressure on Patch #1**



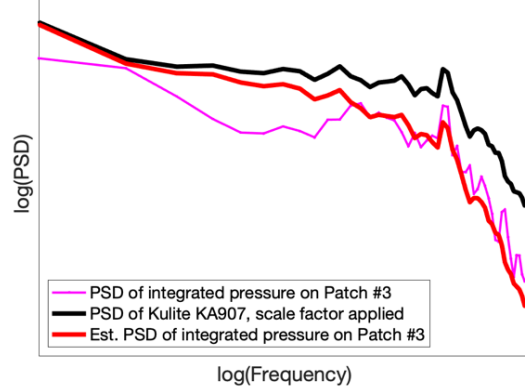
(a)

**SLS AUAT: Mach=0.95, $\alpha=0.0\text{deg}$, $\beta=0.0\text{deg}$
PSD and Est. PSD of Integrated Pressure on Patch #2**



(b)

**SLS AUAT: Mach=0.95, $\alpha=0.0\text{deg}$, $\beta=0.0\text{deg}$
PSD and Est. PSD of Integrated Pressure on Patch #3**



(c)

Fig. 8 PSD of integrated pressure of uPSP measurements and estimated PSD of integrated pressure on Patches #1, #2 and #3, shown in the subplots (a), (b) and (c) respectively, of the SLS AUAT configuration with Mach number 0.95, angle of attack 0.0 degree and angle of sideslip 0.0 degree